Atmos. Chem. Phys. Discuss., 8, 15997–16025, 2008
www.atmos-chem-phys-discuss.net/8/15997/2008/

Atmospheric Chemistry and Physics Discussions

This discussion paper is/has been under review for the journal *Atmospheric Chemistry and Physics (ACP)*. Please refer to the corresponding final paper in *ACP* if available.

Ship emitted NO_2 in the Indian Ocean: comparison of model results with satellite data

K. Franke[1,2], **A. Richter**[1], **H. Bovensmann**[1], **V. Eyring**[2], **P. Jöckel**[3], **and J. P. Burrows**[1]

[1]University of Bremen, Institute for Environmental Physics, Bremen, Germany
[2]Deutsches Zentrum für Luft- und Raumfahrt, Institut für Physik der Atmosphäre, Oberpfaffenhofen, Germany
[3]Max Planck Institute for Chemistry, Mainz, Germany

Received: 25 July 2008 – Accepted: 29 July 2008 – Published: 21 August 2008

Correspondence to: K. Franke (klaus.franke@iup.physik.uni-bremen.de)

Published by Copernicus Publications on behalf of the European Geosciences Union.

Abstract

An inventory of NO_x emission from international shipping has been evaluated by comparing NO_2 tropospheric columns derived from the satellite instruments SCIAMACHY (January 2003 to February 2008), GOME (January 1996 to June 2003), and GOME-2 (March 2007 to February 2008) to NO_2 columns calculated with the atmospheric chemistry general circulation model ECHAM5/MESSy1 (January 2000 to October 2005). The data set from SCIAMACHY yields the first monthly analysis of ship induced NO_2 enhancements in the Indian Ocean. For both data and model consistently the tropospheric excess method was used to obtain mean NO_2 columns over the shipping lane from India to Indonesia, and over two ship free regions, the Bay of Bengal and the central Indian Ocean. In general, the model simulates the differences between the regions affected by ship pollution and ship free regions reasonably well. Minor discrepancies between model results and satellite data were identified during biomass burning seasons in March to May over India and the Indochinese Peninsula and August to October over Indonesia. We conclude that the NO_x ship emission inventory used in this study is a good approximation of NO_x ship emissions in the Indian Ocean for the years 2002 to 2007. It assumes that around 6 Tg(N) yr^{-1} are emitted by international shipping globally, resulting in 90 Gg(N) yr^{-1} in the region of interest when using Automated Mutual Assistance Vessel Rescue System (AMVER) or 72 Gg(N) yr^{-1} when using the International Comprehensive Ocean-Atmosphere Data Set (ICOADS) as spatial proxy. The results do not support some previously published lower ship emissions estimates of 3–4 Tg(N) yr^{-1} globally, making this study the first that evaluates atmospheric response to NO_x ship emission estimates from space.

1 Introduction

Since the industrial revolution the amount of freight transported by international shipping has continually increased. Being powered by fossil fuel, ships contribute to the

ACPD

8, 15997–16025, 2008

anthropogenic burden of air pollutants. One important pollutant emitted by ships is nitrogen monoxide (NO). In the atmosphere NO reacts with ozone (O_3) to form nitrogen dioxide (NO_2). The sum of NO and NO_2, which is known as NO_x, is pseudo conserved. As NO_x participates in the catalytic production of tropospheric ozone, accurate knowledge of amount and distribution of NO_x is needed to understand and assess the role of ship emissions on tropospheric composition and climate. Recent estimates of the global NO_x emissions from international shipping vary over a large range. The global emission data base EDGAR3.2 includes data for 1995 (Olivier and Berdowsky, 2001), which if scaled to year 2000 values assuming a growth rate of 1.5% yr^{-1}, results in annual NO_x emissions of 3.10 Tg(N), similar to the emission totals published by Corbett et al. (1999) and Endresen et al. (2003). Later estimates vary from 5.93 Tg(N) yr^{-1} (Corbett and Koehler, 2003) to 6.36 Tg(N) yr^{-1} (Eyring et al., 2005) for year 2000. In addition to uncertainties in global emission totals, the knowledge of the spatial distribution is limited. As pointed out by Wang et al. (2008), ship activity patterns estimated by the International Comprehensive Ocean-Atmosphere Data Set (ICOADS) and the Automated Mutual-assistance Vessel Rescue System (AMVER) data set have different spatial and statistical sampling biases. Using these or similar NO_x shipping inventories, models have simulated and investigated the impact of shipping emission on tropospheric ozone (Lawrence and Crutzen, 1999; Kasibhatla et al., 2000; Eyring et al., 2007). Using the EDGAR3.2 dataset, the study by Eyring et al. (2007) shows maximum contributions from shipping to annual mean near-surface O_3 over the North Atlantic (56 ppbv in 2000).

Ship emissions of NO_x have been detected in the marine boundary layer (MBL) in satellite data (Richter et al., 2004; Beirle et al., 2004). These studies showed that the NO_2 enhancement in the shipping lane in the north-eastern Indian Ocean and the Red Sea is unambiguously identified from space. To estimate an emission rate from the satellite NO_2, it is necessary to estimate the lifetime of NO_x. For this purpose, Richter et al. (2004) used OH concentrations calculated by Song et al. (2003) to estimate a lifetime of 5.6 h, whereas Beirle et al. (2004) deduced a mean lifetime of about 1.9–6.0 h

from seasonal changes in the pollutant distribution. Both studies concluded that reasonable agreement exists between the estimate of emissions made using satellite data and that available from emission inventories. However, it is clear that the estimation of lifetime of NO_x is one significant source of uncertainty in this comparison.

An alternative approach to investigate the consistency of emission inventories with NO_2 measurements is to calculate the column or concentration of NO_x levels with atmospheric chemistry models. Kasibhatla et al. (2000) and Davis et al. (2001) used ship emission totals of $3\,Tg(N)\,yr^{-1}$ in global chemistry models and compared them to airborne measurements. They conclude that there is an overestimation of ship induced NO_x in the models and attribute this to the coarse resolution of the models and the uncertainties in the inventories. Eyring et al. (2007) compared the model output of eight global models at the local time of SCIAMACHY overpass to the satellite data of Richter et al. (2004). Although the geographical pattern of tropospheric NO_2 is well reproduced, modelled values of the tropospheric column are higher than those observed by SCIAMACHY over the ocean. The shipping lane in the Indian Ocean is not resolved in these simulations because of the low horizontal resolution in the models (between $5.6^\circ \times 5.6^\circ$ and $2.8^\circ \times 2.8^\circ$) compared to the satellite data ($30 \times 60\,km^2$, i.e. $0.27^\circ \times 0.54^\circ$ at the equator). The study also compares the NO_2 total tropospheric columns to the SCIAMACHY observations without applying the tropospheric excess method to the model output. It has been shown by Lauer et al. (2002) that these two quantities differ.

The goal of this work is a quantitative assessment of the various NO_x ship emission estimates that have been published so far. This is achieved by comparing an extended set of satellite NO_2 data with results of the atmospheric chemistry general circulation model ECHAM5/MESSy1. In order to have a consistent comparison of modeled and measured NO_2 columns, the NO_2 tropospheric excess column has been generated from modelled and measured data sets for the first time in the context of ship emissions. Additionally, satellite data is rescaled to match the coarser resolution of the model. In this manner sources of systematic bias in the two data sets of tropospheric column NO_2 were minimised. Subsequently the behaviour and magnitude of these columns

are analysed and the knowledge of the emissions inventories for the Indian Ocean investigated.

2 Data retrieval and analysis

2.1 Tropospheric NO_2 columns retrieved from space

The tropospheric NO_2 columns are retrieved from measurements of the upwelling solar radiation in nadir viewing geometry by the three spectrometers GOME (Burrows et al., 1999; Richter and Burrows, 2002), SCIAMACHY (Burrows et al., 1995; Bovensmann et al., 1999; Richter et al., 2004), and GOME-2 (which is a somewhat improved Version of GOME, Callies et al., 2000), which fly on board the satellites ERS-2, ENVISAT, and METOP-A, respectively. These satellites are in sun synchronous orbits having equator crossing times of 10:30 a.m., 10:00 a.m., and 09:30 a.m., respectively. GOME provides global data from 1996 to June 2003 having a spatial resolution of $40\times320\,km^2$ and $40\times80\,km^2$. Data from January 2003 to February 2008 for SCIAMACHY having a spatial resolution of $30\times60\,km^2$ and from March 2007 to February 2008 for GOME-2 ($40\times80\,km^2$) are available. Monthly mean values were calculated on a grid of $0.125^\circ\times0.125^\circ$. Table 1 describes some relevant instrumental parameters.

The retrieval approach used to determine NO_2 column from the nadir measurements by the satellite instruments is based on the Differential Optical Absorption Spectroscopy (DOAS) method. This technique determines the NO_2 slant column density, SCD, along the light path through the atmosphere in the spectral window between 425 and 450 nm by separating high frequency molecular signatures from broadband absorption and scattering (Brewer et al., 1973; Noxon, 1975; Platt et al., 1979). In order to retrieve tropospheric amounts of NO_2 the technique known as tropospheric excess method (TEM) has been employed. This relies on the longitudinal homogeneity of the stratospheric column. Comparison of the measurements at a given location with the mean SCD in the region from 180° E to 220° E of the same latitude yields the tropo-

spheric excess SCD. This approach assumes implicitly that tropospheric amount of NO_2 in this reference region is negligible (Fig. 1). The SCD can be converted to a vertical column density (VCD) by division with an Air Mass Factor (AMF). The AMF corrects for the different sensitivity of measurements to absorption in different altitudes, which is determined by the relative penetration depth and depends on the magnitude of the surface spectral reflectance and multiple scattering within the atmosphere. This is of particular importance for absorbers located close to the surface. The resulting tropospheric excess column is denoted as TEC. This method belongs to a family of retrieval approaches called residual techniques. The analysis used is described in Richter et al. (2004), more detailed descriptions of the retrieval method can be found in Richter and Burrows (2002) and in Burrows et al. (1999). The overall accuracy of the retrieved columns is about 34% (Richter et al., 2004).

2.2 Model description

ECHAM5/MESSy1 (hereafter referenced as E5/M1) is an Atmospheric Chemistry General Circulation Model (AC-GCM) (Jöckel et al., 2006). The applied spectral resolution is T42, corresponding to a quadratic-gaussian grid of approximately 2.8°×2.8° in longitude and latitude, respectively. The used model setup has 90 layers on a hybrid-pressure grid reaching up to 0.01 hPa. Details of the E5/M1 simulation S1 that is used in this study are described in Jöckel et al. (2006). In order to be able to directly compare the model results with observations, the model dynamics has been nudged using operational analysis data from the European Centre for Medium-Range Weather Forecasts (ECMWF) from January 2000 to October 2005. The model integration time-step is 900 s. Output has been archived as 5-hourly instantaneous fields. This yields an hourly resolved diurnal cycle within 5 days of integration.

Anthropogenic and natural emissions of NO, CO, SO_2, NH_3 and several hydrocarbon species are taken from the EDGAR3.2FT2000[1] dataset (Olivier et al., 2005). NO_x

[1] http://www.mnp.nl/edgar/model/v32ft2000edgar/docv32ft2000

emissions include anthropogenic sources with an annual emission rate of 31 Tg(N) and biomass burning emissions with an annual emission rate of 9.3 Tg(N) (see electronic supplement to Pozzer et al., 2007)[2]. The contribution of ship emission to total anthropogenic NO_x emissions is 6.3 Tg(N) yr^{-1}, which are spatially distributed according to the AMVER activity pattern (Eyring et al., 2005). For comparison with satellite data the relevant E5/M1 parameters are given in Table 1. The E5/M1 model has been evaluated by comparison to the compiled tropospheric in-situ observations of Emmons et al. (2000) [3] and other observational data. These show that the model simulates tropospheric distributions of NO, HNO_3 and PAN concentrations over the tropical Ocean reasonably well (Jöckel et al., 2006).

As a result of the model output being provided at full hours in universal time for every grid box and the ENVISAT satellite having a local equator crossing time of 10:00 am, the model data between 09:30 a.m. and 10:30 a.m. have been averaged in the regions of the ship emissions and the respective reference sectors. Furthermore, to reduce the effects of the inter-annual variability, a 6 year climatological average (2000–2005) of the model data has been used. Two techniques are applied to derive the tropospheric NO_2 columns from the model output. The first technique is consistent with the TEM employed for satellite data. The total columns are derived by vertically integrating over all layers of the atmosphere. NO_2 TECs are then calculated by subtracting the mean total column at the same latitude in a reference sector over the Pacific from the total column at a given location. These NO_2 columns are hereafter denoted as E5/M1(TEM). In the second approach, the column is calculated by integrating the NO_2 amount over the lowest 20 model layers (approx. up to 200 hPa) and denoted as E5/M1(SUM).

[2] http://www.atmos-chem-phys.net/7/2527/2007/acp-7-2527-2007-supplement.pdf

[3] htpp://gctm.acd.ucar.edu/data/

3 Results and discussion

3.1 Comparison of model and SCIAMACHY data

The shipping lane from the southern tip of the Indian subcontinent to Indonesia in the north eastern Indian Ocean has been selected to verify ship induced NO_x, because here ship traffic is concentrated in a narrow line and other local NO_x emissions are negligible. For a quantitative comparison of the model results and the satellite data three regions (S, B1, and B2) depicted in Fig. 2 are defined. The region S is the region which contains the shipping lane. The region B1 is north of the shipping lane and the region B2 is south of the lane. The regions B1 and B2 are assumed not to be significantly influenced by emissions from shipping. All regions have a longitudinal width of four model grid boxes from 83° E to 94.2° E. The regions B1 and B2 have a latitudinal width of two model boxes: B1 extending from 8.4° N to 14° N and B2 from 5.6° S to the equator. The position of the modelled shipping lane (Fig. 2b) is shifted relative to the observed shipping lane (see below). Therefore the region S is defined as the grid box extending from 2.8° N to 5.6° N. For the satellite data, the region S has a latitudinal width of 2.8° centred around the maximum of the NO_2 enhancement in the given month, as shown by the white line in Fig. 3. NO_x ship emissions in region S are calculated from the global emission totals of Endresen et al. (2003), Corbett and Koehler (2003) and Eyring et al. (2005, 2008[4]) using ship activity patterns from AMVER and ICOADS, see Table 2. In the region S the emissions range from 41 Gg(N) yr^{-1} (Endresen et al., 2003 with ICOADS) to 90 Gg(N) yr^{-1} (Eyring et al., 2005 with AMVER), i.e. depending on the inventory the emission estimate differ by more than a factor of 2.

In Fig. 2, the mean February NO_2 tropospheric column amount, derived from all available SCIAMACHY measurements between 2003 and 2008 is compared to E5/M1

[4]Eyring, V., Isaksen, I. S. A., Berntsen, T., Collins, W. J., Corbett, J. J., Endresen, Ø., Grainger, R. G., Moldanova, J., Schlager, H., and Stevenson, D. S.: Assessment of Transport Impacts on Climate and Ozone: Shipping, Atmos. Environ., in review, 2008.

(TEM) and E5/M1 (SUM). The shipping lane in the satellite data is identified by the region having NO_2 TEC of 10×10^{14} molec cm^{-2} in comparison to the surrounding region, where values of around 2×10^{14} molec cm^{-2} are found. The width of the shipping lane is approximately 1° latitude or 110 km (Fig. 2a).

While the overall agreement with E5/M1 (TEM) data is good, the coarse horizontal resolution of the model becomes apparent (Fig. 2b). As the shipping lane is close to a latitudinal boundary of the model grid cells, the shipping signature in the model data is shifted southward relative to the satellite measurements. Qualitatively, as the model grid box is approximately twice as large as the width of the measured shipping lane the maximum reduces from 10×10^{14} molec cm^{-2} to 5×10^{14} molec cm^{-2}.

The difference between E5/M1 (TEM) and E5/M1 (SUM) is about 2.5×10^{14} molec cm^{-2}, with the satellite data being in better agreement with the E5/M1 (TEM) data. While Fig. 2 only shows February, this is valid for all months. This underlines the importance of choosing a consistent data analysis method for the comparison of model and satellite data. In the following analysis only E5/M1 (TEM) is used.

Figure 3 compares zonal mean (83° E to 94.2° E) NO_2 TEC derived from SCIAMACHY to E5/M1 (TEM) and the AMVER ship activity pattern as a function of time and latitude. The shipping lane is discernible by enhanced values of NO_2 TEC throughout the year in the satellite data (Fig. 3a). However, the latitudinal position of the maximum enhancement varies over the year, being further south in the northern hemispheric winter months and further north in the summer. Additionally, the width of the shipping lane and the magnitude of TEC changes over the year. In January and from July to September the signature of ship emissions on the NO_2 TECs spreads over a larger area and the maximum is less pronounced, never rising above 7.5×10^{14} molec cm^{-2}. In the E5/M1 model results this seasonal pattern cannot be resolved as a result of the coarse model resolution (Fig. 3b). As the ship traffic from AMVER data (Wang et al., 2008) in this region shows no distinct seasonality (Fig. 3c; from AMVER data, Wang et al., 2008), this seasonal variation is attributed to the changing meridional wind pat-

terns over this region. In the summer the wind comes mainly from the south whereas in winter it comes from the north. This seasonal variation was also observed by Beirle et al. (2004) in GOME data. The correlation of the latitude of the maximal NO_2 TEC with the mean meridional wind derived from ECMWF reanalysis data is 0.75, i.e. a reasonable strong correlation. In addition, in the satellite data of NO_2 TEC, a significant seasonality over the Bay of Bengal north of the shipping lane between 8° N and 12° N is observed in the months May and June. The potential sources of this behaviour are discussed below.

3.2 Analysis of NO_2 TEC from the three different instruments

Figure 4 shows the mean NO_2 tropospheric excess column for three different instruments compared to the model output in the selected regions S, B1, and B2. For each month the mean of all available years has been calculated from GOME (8 years), SCIAMACHY (5 years), GOME-2 (1 year), and E5/M1 data (6 years). The standard deviation of the averaged data comprises instrument noise plus atmospheric variability of NO_2 and is depicted as errorbar in Fig. 4. As the local time of model data in the regions is centred around 10:00 LT the most direct comparison is between SCIAMACHY and E5/M1(TEM), reducing potential differences through diurnal variations in NO_x. In general SCIAMACHY and E5/M1 (TEM) are in good agreement. In region B1 SCIAMACHY is somewhat higher than E5/M1 (TEM) in March and May, while in region B2 SCIAMACHY is somewhat higher than E5/M1 (TEM) in September and October. The small discrepancies in region B1 and B2 coincide with the biomass burning seasons in adjacent landmasses as seen in the TRMM Fire Index[5], i.e. typically February to May/June in India and the Indochinese Peninsula and from August to October in Indonesia. As the EDGAR3.2FT2000 dataset is valid for the year 2000 and SCIAMACHY measurements are from 2003 to 2008 discrepancies between model input and actual biomass burning emissions can be expected.

[5] http://tsdis.gsfc.nasa.gov/tsdis/Fire/monthly_archive.html

The GOME and GOME-2 measurements are consistent with SCIAMACHY data within errorbars in the regions S, B1, and B2 throughout the year. One exception is the large value of GOME-2 in January 2008. As the NO_2 TEC measured by SCIAMACHY in January 2008 is also enhanced in comparison to former years (not shown), we concider this to be a result of a special situation occurring in this month. As this deviation happens in all three regions, it is considered not to be related to the ship traffic and is not further discussed in this study. The observation of enhanced NO_2 TEC by all three instruments compared to model results in region B1 in March and May and in region B2 in September and October indicates that they do not result from a bias inherent to SCIAMACHY, but reflect variations in tropospheric NO_2 content.

While monthly means among the satellite instruments are consistent within errorbars, the annual mean NO_2 TEC over the regions S among the instruments differ (Fig. 5). Possible explanations of this difference in TEC NO_2 over region S are

(i) changes of ship emissions over time,

(ii) diurnal variation of NO_2,

(iii) change of background NO_x field.

In the following we will discuss these aspects in more detail.

(i) Over the last 30 years a clear and well understood correspondence is observed between fuel consumption and seaborne trade in ton miles, because the work done in global trade is proportional to the energy required (Eyring et al., 2008[4]). The total seaborne trade volume (STV) has risen from 20 968 tmi (tonne miles) in 1996 to 31 847 tmi in 2007 (Fearnleys, 2007). As no significant measures of NO_x-reductions have been introduced, we use the increase in STV over this period as an indicator for NO_x increase. The rise in STV over the time period covered by GOME measurements (1996–2002) is 15% with a mean STV of 22 549 tmi, while it is a 21% increase with a mean value of 29 021 tmi over the time period of SCIAMACHY observations (2003–2008). The mean STV for the SCIAMACHY measurement time period is 29% higher

ACPD
8, 15997–16025, 2008

than the mean STV for GOME observations, while it is 10% lower than the mean STV of 31 847 tmi during the time period of GOME-2 measurements (2007–2008).

In order to assess the difference in the measurements that is due to the raise in NO_x emissions, linear regression on the monthly mean NO_2 TECs (this time without inter-annual average) was performed. Linear regression over 84 months of GOME measurements in region S yields a slope of $(0.0\pm0.13)\times10^{14}$ molec cm^{-2} yr^{-1}, which corresponds to (0±22)% of the mean NO_2 TEC of all available GOME data. For the 67 month of SCIAMACHY measurements the regression gives a slope of $(0.15\pm0.15)\times10^{14}$ molec cm^{-2} yr^{-1} (14±14%). This implies that no significant trend is discernible within the error of measurement over the periods of measurements of either GOME or SCIAMACHY. However, the change in mean NO_2 TEC between the measurement periods of GOME and SCIAMACHY has increased by (26±15)%, which is in agreement with the rise of 29% in STV (Fig. 5). On the other hand, the mean NO_2 TEC as observed by GOME-2 from 2007 to 2008 is (37±22)% higher than the mean NO_2 TEC over the period of measurement of SCIAMACHY (2003–2008), which is substantially higher than what would be expected from the 10% rise of the mean STV.

(ii) The diurnal variation of NO_2 arises from variation of its photodissociation rate and the effective first order removal rate for its reaction with OH. As a result of these two processes NO_2 decreases during the morning. As the equator crossing times of GOME-2, SCIAMACHY and GOME are 09:30, 10:00, and 10:30 LT, respectively, the instruments see different parts of this diurnal cycle. To investigate whether the observed differences can be explained by the diurnal cycle, the mean NO_2 TECs from GOME and SCIAMACHY are compared for the period August 2002 to June 2003 and for the period March 2007 to February 2008 for SCIAMACHY and GOME-2. By confining the analysis on these time periods the seasonal and inter-annual variation is removed from the data. In addition, the diurnal variation between 09:30 a.m. and 10:00 a.m. and between 10:00 a.m. and 10:30 a.m. in mean NO_2 TEC in region S is calculated from all E5/M1 (TEM) results.

Over the region S the model predicts a decrease in mean NO_2 TEC of 0.6–0.7×10^{14} molec cm^{-2} over the half of an hour between the respective equator crossing times (Fig. 6). However, the difference in mean NO_2 TEC derived from GOME and SCIAMACHY measurements from 2002/2003 show no significant decrease over this half hour (green data in Fig. 6). On the other hand, the difference in mean NO_2 TEC measured by GOME-2 and SCIAMACHY in 2007/2008 is about $(1.6\pm1.4)\times10^{14}$ molec cm^{-2} in region S, and therefore greater than predicted by the model (blue data in Fig. 6). In conclusion, the differences among the three satellite instruments cannot be explained by the diurnal variaion, as the difference between GOME and SCIAMACHY that measure at 10:30 a.m. and 10:00 a.m. repsectively is smaller than expected from the model while the difference between SCIAMACHY and GOME-2 (09:30 a.m.) is larger.

In conclusion of this section, the different satellite instruments measure different mean NO_2 TECs over region S. While the difference between GOME and SCIAMACHY is consistent with the rise in STV, no diurnal variation could be identified in the time period of overlapping measurements of GOME and SCIAMACHY. On the other hand, the difference in NO_2 TEC between GOME-2 and SCIAMACHY is greater than expected from either diurnal variation of NO_2 or rise in NO_x ship emissions. Another explanation could be a change in background NO_x levels due to a change of outflow of NO_x from adjacent landmasses (Kunhikrishnan and Lawrence, 2004). As a detailed assessment of these influences from adjacent landmasses requires additional data of continental sources and also is not related to the main topic of this paper on ship induced NO_2 changes over the Indian Ocean it is not further pursued.

3.3 Evaluation of ship emission inventories

So far we could show that the model agrees reasonably well with the satellite data. As the NO_2 level over the ship influenced region S comprises ship induced and background NO_x, the difference between the ship polluted area S and the two shipfree

background regions B1 and B2 is determined, to see if there is a significant overestimation of ship induced NO_x in the model simulation. Overestimation could result because in the model simulation one of the higher NO_x estimates for international shipping has been used (see Table 2 for comparison), and because plume processing has been neglected, which could lead to different NO_x lifetimes inside the plume (Franke et al., 2008). However, the model results and the measurements agree well in the difference between regions S and B1 with the exception of May (Fig. 7, upper panel). This has its origin in the high value in B1 in this month (Fig. 4) and is therefore not related to ship emissions. Differences between S and B1 show an annual cycle with a minimum of 0.5×10^{14} molec cm^{-2} in August and a maximum of 4×10^{14} molec cm^{-2} in April. The correlation between the two curves is 0.87 (0.95 excluding May). The difference between S and B2 shows no significant annual cycle, and the model results and the satellite data are close to 5×10^{14} molec cm^{-2} (Fig. 7, lower panel).

The agreement between model results and satellite data is more obvious in Fig. 8. Here the differences in NO_2 TEC between the regions from model output are plotted against those from GOME and SCIAMACHY. SCIAMACHY values for S-B1 are all (with the exception of the May value) located near the 1:1 line showing again the high correlation and also the absence of a significant bias. The S-B2 differences centre also on the bisecting line, showing no discernable correlation, but also no bias (Fig. 8, lower panel). On the other side, GOME values are slightly lower, being left of the 1:1 line.

The ship inventory by Eyring et al. (2005) applied in the model simulation results in emission totals of 90 Gg(N) yr^{-1} in region S. As discussed earlier, other emission inventories give around half of this amount even if scaled with the increase of total seaborne trade to the year 2005, see Table 2. If we assume linear relation between simulated NO_2 and emitted NO_x as a simple approximation, with half the NO_x emissions the model would predict an NO_2 enhancement half as high as with the current model results. This corresponds to the 1:2 line in Fig. 8. As the measurements are close to the 1:1 line, this simple comparison favours the inventory used here and shows that some previously published lower ship emissions estimates of 3–4 Tg(N) yr^{1} combined

ACPD
8, 15997–16025, 2008

with either AMVER or ICOADS are too low in comparison to the satellite data.

4 Conclusions

Ship emissions of NO_x in the Indian Ocean have been analysed with the help of measurements from GOME (1996–2002), SCIAMACHY (2003–2007), and GOME-2 (2007/2008) in comparison to a global model simulation. The Differential Optical Absorption Spectroscopy (DOAS) method and the tropospheric excess method (TEM) were used to retrieve NO_2 tropospheric excess columns (TECs) in the northern Indian Ocean. The satellite data was compared to NO_2 TEC retrieved from the output of a nudged simulation with the atmospheric chemistry general circulation model ECHAM5/MESSy1 (2000–2005). The shipping route from India to Indonesia can be detected in satellite data with an enhancement in NO_2 TEC of about 8×10^{14} molec cm^{-2}. A monthly variation of the latitudinal position of the NO_2 enhancement could be identified with a correlation of 0.75 between the latitudinal position of the maximal NO_2 enhancement and mean meridional wind speed derived from ECMWF reanalysis data.

For detailed analysis three regions were defined, one including the shipping lane (S), one in the Bay of Bengal (B1) and one over the free Indian Ocean (B2). B1 and B2 are assumed not to be influenced by ship emissions. Overall comparison of SCIAMACHY NO_2 TEC and E5/M1 TEC in the defined regions shows good agreement with SCIAMACHY being somewhat higher in B2 in August to November and somewhat higher in S and B1 in March and May. These differences in NO_2 TEC coincide with biomass burning seasons on landmasses nearby, i.e. February to May over India and the Indochinese Peninsula and August to October over Indonesia.

An analysis of differences between mean NO_2 TEC values in region S shows that GOME-2 has a $(2\pm1)\times10^{14}$ molec cm^{-2} higher TEC than SCIAMACHY. In comparison the NO_2 TEC as measured by GOME and SCIAMACHY differs by $(1.1\pm0.6)\times10^{14}$ molec cm^{-2}. Two effects with possible contributions to these differ-

ences were analysed: First, the diurnal cycle of NO_2 as the three instruments measure NO_2 at slightly different times during the day (GOME-2 at 09:30 a.m.; SCIAMACHY at 10:00 a.m.; GOME at 10:30 a.m.), and second, the change in NO_x ship emissions over the measurement period. The diurnal variation could not unambiguously identified in the satellite data, because the standard deviation of the measurements is greater than the change in NO_2 TEC as calculated by the model. Some of the difference can be attributed to the difference in the measurement period as ship emissions in the shipping lanes from 1996 to 2007 are expected to have increased. Linear Regression has been used to study the trend in NO_2 TEC within the measurement period from either GOME or SCIAMACHY. For this trend analysis no significant change greater than the standard deviation could be identified. However, the difference of (26±15)% in mean NO_2 TEC between satellite measurements by GOME and SCIAMACHY is consistent with the rise of 29% in mean seaborne trade volume.

Finally, the ship induced NO_2 enhancement was derived from the difference between NO_2 TEC in the ship influenced region S and the ship free regions B1 and B2. Here, agreement between satellite data and model results is very good with a correlation of 0.87. In addition, a simple linear estimation of results expected from using emission data with half the NO_x flux give significantly lower estimations of ship induced change in NO_2 TEC over the Indian Ocean. Therefore we conclude, that a ship emission inventory with around 6 Tg(N) yr^{-1} globally resulting in around 90 Gg(N) yr^{-1} in the region of interest when using the Automated-Mutual-Assistance Vessel Rescue System (AMVER) or around 72 Gg(N) yr^{-1} when using the International Comprehensive Ocean-Atmosphere Data Set (ICOADS) as spatial proxy provides better agreement with measurement in the Indian Ocean than previously published lower ship emissions estimates of 3–4 Tg(N) yr^{-1} globally. A more extensive comparison of the ship emission inventories on the global scale would be necessary to further strengthen this result.

Acknowledgements. This work has been supported by the Helmholtz-University Young Investigators Group SeaKLIM, which is funded by the Helmholtz Association of German Research Centres and the German Aerospace Centre (DLR). It has also been supported by the University

and State of Bremen and the EU ACCENT network. We would like to thank Ulrike Burkhardt for her comments on the manuscript.

References

Beirle, S., Platt, U., von Glasow, R., Wenig, M., and Wagner, T.: Estimate of nitrogen oxide emissions from shipping by satellite remote sensing, Geophys. Res. Lett., 31, L18102, doi:10.1029/2004GL020312, 2004. 15999, 16006

Bovensmann, H., Burrows, J., Buchwitz, M., Frerick, J., Noël, S., Rozanov, V., Chance, K., and Goede, A.: SCIAMACHY: Mission Objectives and Measurement Modes, J. Atmos. Sci., 56, 127–150, 1999. 16001

Brewer, A., McElroy, C., and Kerr, J.: Nitrogen dioxide concentrations in the atmosphere, Nature, 246, 129–133, 1973. 16001

Burrows, J., Hölzle, E., Goede, A., Visser, H., and Fricke, W.: SCIAMACHY—scanning imaging absorption spectrometer for atmospheric chartography, Acta Astronaut., 35, 445–451, 1995. 16001

Burrows, J., Weber, M., Buchwitz, M., et al.: The Global Ozone Monitoring Experiment (GOME): Mission Concept and First Scientific Results, J. Atmos. Sci., 56, 151–175, 1999. 16001, 16002

Callies, J., Corpaccioli, E., Eisinger, M., Hahne, A., and Lefebvre, A.: GOME-2- Metop's second-generation sensor for operational ozone monitoring, ESA Bull., 102, 28–36, 2000. 16001

Corbett, J., Fischbeck, P., and Pandis, S.: Global nitrogen and sulfur inventories for oceangoing ships, J. Geophys. Res., 104, 3457–3470, 1999. 15999

Corbett, J. J. and Koehler, H. W.: Updated emissions from ocean shipping, J. Geophys. Res., 108, 4650, 2003. 15999, 16004, 16017

Davis, D., Grodzinsky, G., Kasibhatla, P., Crawford, J., Chen, G., Liu, S., Bandy, A., Thornton, D., Guan, H., and Sandholm, S.: Impact of ship emissions on marine boundary layer NO_x and SO_2 distributions over the Pacific basin, Geophys. Res. Lett., 28, 235–238, 2001. 16000

Emmons, L., Hauglustaine, D., Mueller, J., Carroll, M., Brasseur, G., Brunner, D., Staehelin, J., Thouret, V., and Marenco, A.: Data composites of airborne observations of tropospheric ozone and its precursors, J. Geophys. Res., 105, 20 497–20 538, 2000. 16003

Endresen, Ø., Sørgård, E., Sundet, J., Dalsøren, S., Isaksen, I., Berglen, T., and Gravir, G.: Emission from international sea transportation and environmental impact, J. Geophys. Res., 108, 4560, 2003. 15999, 16004, 16017

Eyring, V., Köhler, H. W., van Aardenne, J., and Lauer, A.: Emissions from international shipping: 1. The last 50 years, J. Geophys. Res., 110, D17305, doi:10.1029/2004JD005619, 2005. 15999, 16003, 16004, 16010, 16016, 16017, 16018

Eyring, V., Stevenson, D. S., Lauer, A., Dentener, F. J., Butler, T., Collins, W. J., Ellingsen, K., Gauss, M., Hauglustaine, D. A., Isaksen, I. S. A., Lawrence, M. G., Richter, A., Rodriguez, J. M., Sanderson, M., Strahan, S. E., Sudo, K., Szopa, S., van Noije, T. P. C., and Wild, O.: Multi-model simulations of the impact of international shipping on Atmospheric Chemistry and Climate in 2000 and 2030, Atmos. Chem. Phys., 7, 757–780, 2007, http://www.atmos-chem-phys.net/7/757/2007/. 15999, 16000

Fearnleys: Fearnleys Review 2007, The Tanker and Bulk Markets and Fleets, Tech. Rep., Oslo, 2007. 16007

Franke, K., Eyring, V., Sander, R., Hendricks, J., Lauer, A., and Sausen, R.: Toward effective emissions of ships in global models, Meteorol. Z., 17, 117–129, 2008. 16010

Jöckel, P., Tost, H., Pozzer, A., Brühl, C., Buchholz, J., Ganzeveld, L., Hoor, P., Kerkweg, A., Lawrence, M., Sander, R., Steil, B., Stiller, G., Tanarhte, M., Taraborrelli, D., van Aardenne, J., and Lelieveld, J.: The atmospheric chemistry general circulation model ECHAM5/MESSy1: consistent simulation of ozone from the surface to the mesosphere, Atmos. Chem. Phys., 6, 5067–5104, 2006, http://www.atmos-chem-phys.net/6/5067/2006/. 16002, 16003

Kasibhatla, P., Levy, H., Moxim, W., Pandis, S., Corbett, J., Peterson, M., Honrath, R., Frost, G., Knapp, K., Parrish, D., and Ryerson, T.: Do emissions from ships have a significant impact on concentrations of nitrogen oxides in the marine boundary layer?, Geophys. Res. Lett., 27, 2229–2232, 2000. 15999, 16000

Kunhikrishnan, T. and Lawrence, M.: Sensitivity of NO_x over the Indian Ocean to emissions from the surrounding continents and nonlinearities in atmospheric chemistry responses, Geophys. Res. Lett., 31, L15109, doi:10.1029/2004GL020210, 2004. 16009

Lauer, A., Dameris, M., Richter, A., and Burrows, J. P.: Tropospheric NO_2 columns: a comparison between model and retrieved data from GOME measurements, Atmos. Chem. Phys., 2, 67–78, 2002, http://www.atmos-chem-phys.net/2/67/2002/. 16000

Lawrence, M. and Crutzen, P.: Influence of NO_x emissions from ships on tropospheric photo-

chemistry and climate, Nature, 402, 167–170, 1999. 15999
Noxon, J.: Nitrogen dioxide in the stratosphere and tropsphere as measured by ground-based absoption spectroscopy, Science, 189, 547–549, 1975. 16001
Olivier, J. and Berdowsky, J.: Global emission sources and sinks, in: The Climate System, edited by: Berdowski, J., Guicherit, R., and Heij, B., 33–77, A. A. Balkema Publishers/Swets & Zeitlinger Publishers, Lisse, The Netherlands, 2001. 15999
Olivier, J. G. J., van Aardenne, J. A., Dentener, F., Ganzeveld, L., and Peters, J. A. H. W.: Recent trends in global greenhouse gas emissions: regional trends and spatial distribution of key sources, in: Non-CO2 Greenhouse Gases (NCGG-4), edited by: van Amstel, A., 325–330, Millpress, Rotterdam, ISBN 90 5966 043 9, 2005. 16002
Platt, U., Perner, D., and Pätz, H.: Simultaneous measurement of atmospheric CH2O, O_3, and NO 2 by differential optical absorption, J. Geophys. Res., 84, 6329–6335, 1979. 16001
Pozzer, A., Jöckel, P., Tost, H., Sander, R., Ganzeveld, L., Kerkweg, A., and Lelieveld, J.: Simulating organic species with the global atmospheric chemistry general circulation model ECHAM5/MESSy1: a comparison of model results with observations, Atmos. Chem. Phys., 7, 2527–2550, 2007, http://www.atmos-chem-phys.net/7/2527/2007/. 16003
Richter, A. and Burrows, J.: Tropospheric NO_2 from GOME measurements, Adv. Space Res., 29, 1673–1683, 2002. 16001, 16002
Richter, A., Eyring, V., Burrows, J., Bovensmann, H., Lauer, A., Sierk, B., and Crutzen, P.: Satellite measurements of NO_2 from international shipping emissions, Geophys. Res. Lett., 31, L23110, doi:10.1029/2004GL020822, 2004. 15999, 16000, 16001, 16002
Song, C., Chen, G., Hanna, S., Crawford, J., and Davis, D.: Dispersion and chemical evolution of ship plumes in the marine boundary layer: Investigation of $O_3/NO_y/HO_x$ chemistry, J. Geophys. Res., 108, 4143, doi:10.1029/2002JD002216, 2003. 15999
Wang, C., Corbett, J., and Firestone, J.: Improving Spatial Representation of Global Ship Emissions Inventories, Environ. Sci. Technol., 42, 193–199, 2008. 15999, 16005, 16020

Table 1. Important parameters of the used satellite data and the model.

	Covered Period	Local Time	Resolution (km^2)
GOME	1996–2002	10:30	40×320
SCIAMACHY	2003–2008	10:00	30×60
GOME-2	2007–2008	09:30	40×80
E5/M1	2000–2005[a] (2001)[b]	09:30–10:30	2.8°×2.8°

[a]Period of used ECMWF data.
[b]The used ship emission inventory is calculated for the year 2001 (Eyring et al., 2005).

Table 2. NO_x ship emissions from existing literature. The table summarizes the global emission total and the emission into region S (83° E–94.2° E/4.4° N–7.2° N) for different spatial ship activity patterns (AMVER and ICOADS). Emission rates for 2000 are scaled with the increase of total seaborne trade to the year 2005.

	2000 NO_x emissions in Tg(N) yr^{-1}			2005 NO_x emissions in Tg(N) yr^{-1}		
	Global	S (AMVER)	S (ICOADS)	Global	S (AMVER)	S (ICOADS)
Endresen et al. (2003)	3.63	0.052	0.041	4.45	0.063	0.050
Corbett and Koehler (2003)	5.93	0.084	0.067	7.28	0.103	0.082
Eyring et al. (2005)	6.36	0.090	0.072	7.81	0.111	0.088
Eyring et al. (2008)[4]	5.18	0.074	0.059	6.36	0.090	0.072

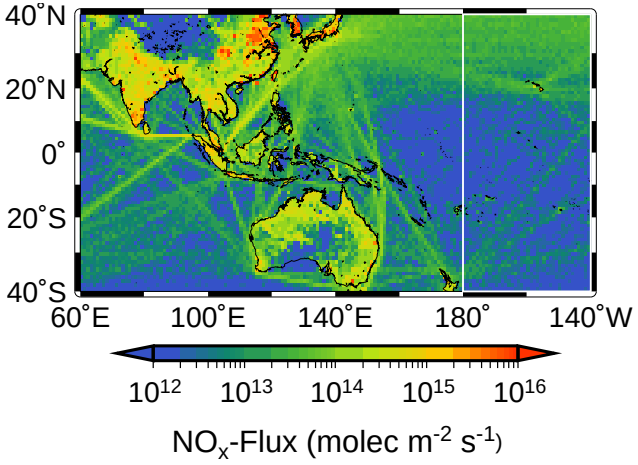

Fig. 1. NO_x emissions inventory as used in the model simulation. Estimates are taken from EDGAR3.2FT2000 over land and from Eyring et al. (2005) for ship emissions. The reference sector used in the tropospheric excess method (TEM) from 180°to 140° W is marked by the white box.

ACPD
8, 15997–16025, 2008

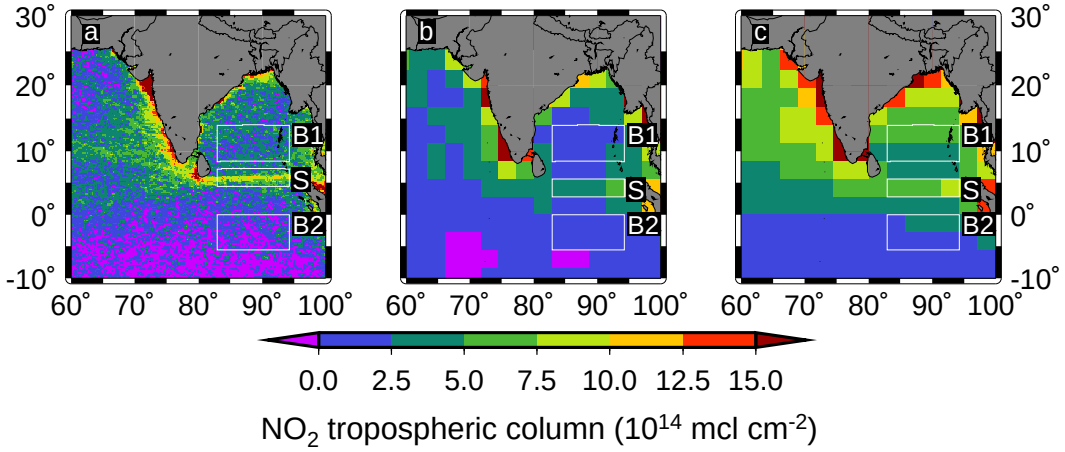

Fig. 2. February mean tropospheric NO_2 columns: **(a)** derived from SCIAMACHY measurements from 2003 to 2008 using the DOAS technique and the tropospheric excess method (TEM). **(b)** taken from the E5/M1 model using the TEM. **(c)** taken from the E5/M1 model integrating the NO_2 concentration up to approximately 200 hPa (SUM). The white boxes indicate the averaging regions used for further comparison.

ACPD
8, 15997–16025, 2008

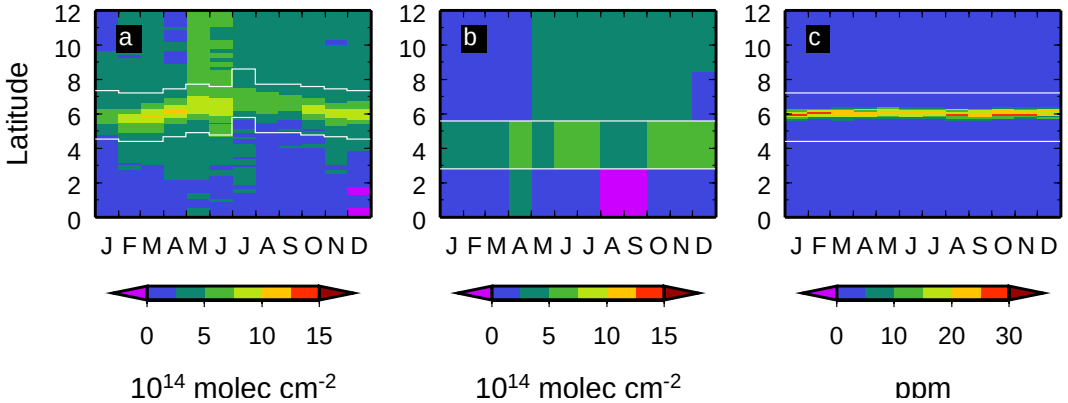

Fig. 3. Monthly zonal mean NO_2 tropospheric excess columns **(a)** derived from SCIAMACHY measurements from 2003 to 2008 using the DOAS technique and the tropospheric excess method (TEM); **(b)** derived from ECHAM5/MESSy1 model simulations from 2000 to 2005 and the TEM. **(c)** Zonal mean AMVER ship activity measured in ppm of global ship traffic (Wang et al., 2008). The zonal average includes data from 83° E to 94.2° E. White lines indicate the northern and southern border of region S.

ACPD
8, 15997–16025, 2008

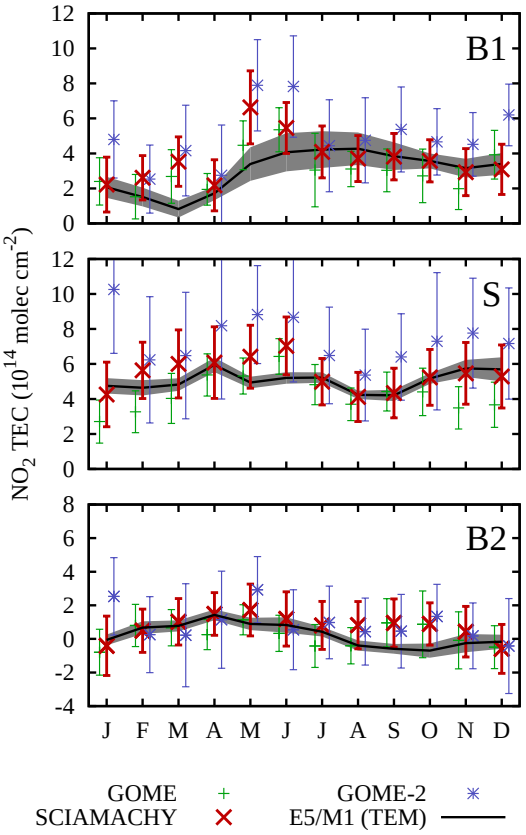

Fig. 4. Monthly mean NO_2 tropospheric column in three selected regions over the Indian Ocean. Satellite data from SCIAMACHY, GOME and GOME-2 are denoted by symbols. For model output columns are derived by tropospheric excess method (TEM).

ACPD
8, 15997–16025, 2008

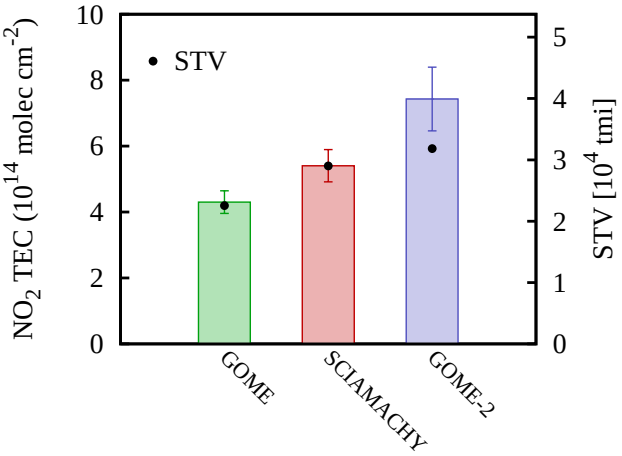

Fig. 5. Multiannual mean NO_2 tropospheric excess column (TEC) measured with satellite instruments GOME(1996–2003), SCIAMACHY(2002–2008), and GOME-2 (2007–2008) over region S over the Indian Ocean. In addition, the mean seaborne trade volume (STV) over the corresponding time periods is given (•).

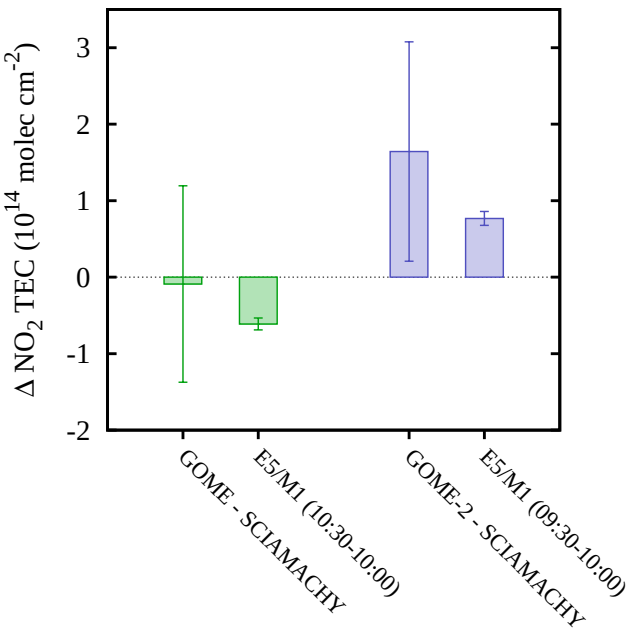

Fig. 6. Difference in mean NO_2 TEC (ΔNO_2 TEC) as a result of diurnal variation in tropospheric NO_2 over the region S estimated from satellite measurements compared to the corresponding ΔNO_2 TEC from model simulations. The differences in NO_2 TEC between GOME (10:30 a.m.) and SCIAMACHY (10:00 a.m.) measurements are calculated for the period from August 2002 to June 2003. The differences in NO_2 TEC between GOME-2 (09:30 a.m.) and SCIAMACHY (10:00 a.m.) measurements are calculated for the period from March 2007 to February 2007.

ACPD
8, 15997–16025, 2008

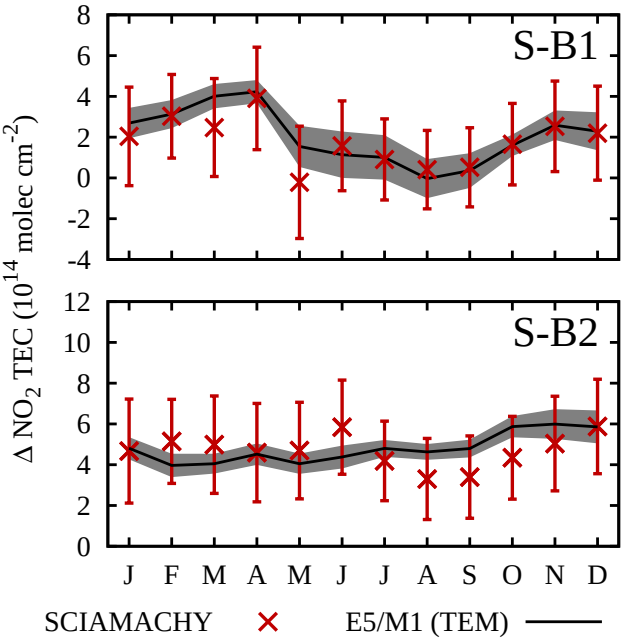

Fig. 7. Difference in NO_2 tropospheric column over the shipping lane from India to Indonesia to NO_2 over the Bay of Bengal (S-B1) and over the central Indian Ocean (S-B2). Data from SCIAMACHY and the model E5/M1 are shown as a function of time.

ACPD
8, 15997–16025, 2008

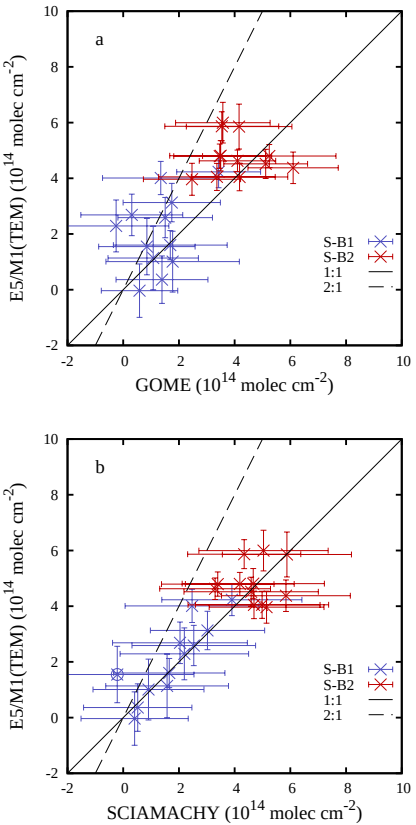

Fig. 8. Difference in NO_2 tropospheric column over the shipping lane from India to Indonesia to NO_2 over the Bay of Bengal (S-B1) and over the central Indian Ocean (S-B2). Data from **(a)** GOME and **(b)** SCIAMACHY are correlated to output from the model E5/M1. The SCIAMACHY value marked with the circle corresponds to the month of May.